Geological Survey of Canada

CURRENT RESEARCH 2001-E4

Reconnaissance gamma-ray spectrometry studies of the Paleoproterozoic Piling Group and adjacent Archean basement rocks, central Baffin Island, Nunavut

K.L. Ford

Natural Resources Canada

Ressources naturelles Canada

Canadä

Reconnaissance gamma-ray spectrometry studies of the Paleoproterozoic Piling Group and adjacent Archean basement rocks, central Baffin Island, Nunavut

K.L. Ford

Mineral Resources Division, Ottawa

Abstract

In the southern Melville Peninsula, strong radioactive element patterns, measured by reconnaissance airborne gamma-ray spectrometry, clearly discriminate Archean orthogneiss and various Archean and Proterozoic plutonic rocks. Similar geological units occur in the central Baffin Island region. In 2000, a brief field study was conducted in central Baffin Island to determine if radioactive element (K, eU, and eTh) variations measured by ground gamma-ray spectrometry can be used to assist ongoing geological mapping activities.

Although radioactive element concentrations are generally low in the supracrustal rocks of the Piling Group, variation in K and eTh concentrations are associated with lithological variations. Basement rocks, composed of Archean orthogneiss and various Archean and Proterozoic granitic intrusions, produce strong radioactive element contrasts. Young pegmatite plutons can be distinguished from older intrusions by low eTh concentrations and high eU/eTh ratios. Various Archean and Proterozoic intrusions also have characteristic radioactive element signatures which distinguish them from Archean orthogneiss.

Résumé

Dans le sud de la presqu'île Melville, les configurations très bien définies des concentrations d'éléments radioactifs mesurées lors de levés aériens de spectrométrie gamma de reconnaissance permettent de différencier très aisément les orthogneiss de l'Archéen des autres roches plutoniques de l'Archéen et du Protérozoïque. Des unités géologiques semblables sont présentes dans la partie centrale de l'île de Baffin. En l'an 2000, une rapide étude de terrain a été effectuée dans cette région afin de déterminer si les variations des concentrations des éléments radioactifs (K, eU et eTh) mesurées à l'aide de levés au sol de spectrométrie gamma pouvaient servir d'appui aux travaux de cartographie géologique actuellement en cours.

Bien que les concentrations d'éléments radioactifs soient généralement faibles dans les roches supracrustales du Groupe de Piling, la variation des concentrations de K et de eTh peut y être associée aux variations lithologiques. Les roches du socle, composées d'orthogneiss de l'Archéen et de diverses intrusions granitiques de l'Archéen et du Protérozoïque, affichent des signatures très contrastées quant aux concentrations d'éléments radioactifs. De faibles concentrations de eTh et des rapports eU/eTh élevés permettent de différencier les plutons de pegmatite de formation récente des intrusions plus anciennes. Diverses intrusions de l'Archéen et du Protérozoïque présentent également des signatures caractéristiques quant aux concentrations d'éléments radioactifs qui permettent de les différencier des orthogneiss de l'Archéen.

INTRODUCTION

In 2001, a three-year multidisciplinary, multiagency project was initiated to investigate the Archean basement rocks and overlying Paleoproterozoic supracrustals of the Piling Group in the central Baffin Island region of Nunavut. The bedrock mapping component of this project was reported by Corrigan et al. (2001). Elsewhere, in the southern Melville Peninsula, similar bedrock units produce very strong

radioactive element contrasts in reconnaissance airborne gamma-ray spectrometry surveys (Holman et al., in press). This suggests airborne and ground-spectrometry techniques offer support for ongoing and future geological mapping and exploration activities in both regions.

In August 2001, a two-week ground gamma-ray spectrometry study was conducted in central Baffin Island to determine if radioactive element contrasts within the Archean basement and overlying supracrustal rocks of the Piling Group are sufficient to assist bedrock mapping. This paper summarizes initial results to date.

GAMMA-RAY SPECTROMETRY

Gamma-ray spectrometry surveys have an obvious and significant role to play in regional and detailed bedrock and surficial geological mapping programs, mineral exploration for a wide variety of commodities (rare, base, and precious metals, granophile elements and industrial minerals), environmental radiation monitoring, and land-use planning (Shives et al., 1995, 1997; Ford et al., in press). In Canada and elsewhere numerous examples show that gamma-ray spectrometry provides important information by mapping the radioactive element characteristics of various lithologies in complex terrains (Darnley and Ford, 1989; Charbonneau et al., 1997). In Australia Wilford et al. (1997) demonstrated that airborne gamma-ray spectrometry patterns provided important information for soil, regolith, and geomorphology studies used for land management and mineral exploration decisions.

These airborne and ground surveys are successful because they employ sensitive, properly calibrated detector systems that provide accurate estimates of ground concentrations of the three most common, naturally occurring radioactive elements, potassium, uranium, and thorium. The technique is ideally suited to map radioactive element concentrations of granitic and gneissic terrains because of the

generally higher contrasts (Killeen, 1979) exhibited by these lithologies. Although sedimentary terrains typically have low abundances of K, U, and Th, (Killeen, 1979), detailed ground surveys and borehole radioactivity logs commonly distinguish different lithologies through variations in the concentration of thorium- or potassium-bearing minerals (Mwenifumbo et al., 2000). Therefore, given sufficient sensitivity and ground control, even minor radioactive element variations can be delineated.

METHODOLOGY

All ground gamma-ray spectrometry measurements were made using an Exploranium GR320 spectrometer with a 0.35 L NaI detector and a counting time of 120 seconds. The detector and console weigh approximately 7.6 kg and are carried in a backpack. Before each field season, the spectrometer is calibrated on concrete pads containing known concentrations of K, U, and Th. This calibration provides the stripping ratios and sensitivities required by the spectrometer and supporting software to display properly corrected estimates of K, equivalent U, and equivalent Th in real time. The term 'equivalent' or its abbreviation 'e' is used to indicate that equilibrium is assumed between the radioactive daughter isotope monitored by the spectrometer, and its respective parent isotope. For ^{238}U, gamma rays emitted by ^{214}Bi at 1.76 MeV are measured and for ^{232}Th, gamma rays emitted by ^{208}Tl at 2.41 MeV are measured. Within the detector, an internal ^{137}Cs source allows the spectrometer to automatically maintain system stability. In the field, results are displayed in real time as concentrations of each radioactive element. All measurements are stored by the spectrometer as 256-channel spectra for downloading daily to a computer for further analysis, if required. To improve results, changes in local background radiation are monitored by periodically taking measurements over a large body of water, at least 100 m from shore. A total-count scintillometer was used to continuously monitor changes in total radioactivity. This ensures that sites selected for a spectrometric measurement are representative, and that anomalous areas are not

overlooked. Where appropriate, several spectrometer measurements may be made in close proximity to determine if systematic variations in the individual radioactive element concentrations correlate with subtle variations in total radioactivity or with recognizable lithological characteristics.

Positional data were gathered using a Trimble GeoExplorer II. Magnetic susceptibility measurements were also collected at each site using an Exploranium KT-5 digital magnetic susceptibility meter. For this study, all spectrometer measurements were made on large bedrock exposures that provide flat, 2-pi geometry (**Fig. 1**), as required by calibration procedures. Small or angular exposures, providing less than or greater than 2-pi geometry, were avoided.

INITIAL RESULTS

Preliminary evaluation of results from 230 ground gamma-ray spectrometry measurements indicates several radioactive element trends within the area studied. Generalized traverse and site locations are shown on a simplified geological map (**Fig. 2**) of part of the Foxe Fold Belt on central Baffin Island (Corrigan et al., 2001). The main transect comprises four traverses (A, B, C, D, Fig. 2) across the central part of the upper sequence of the Piling Group, composed of psammite, pelite, wacke, and minor calc-silicate of the Longstaffe Bluff Formation (Corrigan et al., 2001). Traverse E (Fig. 2) started in a biotite syenogranite, crossed the lower sequence of the Piling Group, composed of quartzite and psammite of the Dewar Lake Formation, and marble and calc-silicate rock of the Flint Lake Formation, and terminated in psammite of the Longstaffe Bluff Formation. The last traverse (F, Fig. 2) started in the central part of a large pegmatite intrusion and crossed into psammite of the Longstaffe Bluff Formation. In addition to these six traverses, five individual site locations (S1–S5, Fig. 2) were also visited where multiple spectrometer measurements were collected. These five sites are located north of the Piling Group in the

Archean basement, composed of variably deformed and metamorphosed felsic plutonic rocks and migmatite (S1, S4, and S5, **Fig. 2**), banded granitic and tonalitic gneiss (S2, Fig. 2), and megacrystic monzogranite (S3, Fig. 2).

The mean, standard deviation, and range of K, eU, and eTh concentrations for all 230 gamma-ray spectrometry measurements are presented in **Tables 1**, **2**, and **3**, grouped separately according to the major lithological units determined in the field. The XY plots of all the spectrometry measurements for each lithological unit are presented in **Figures 3**, **4**, and **5** as eTh versus K, eU versus eTh, and/or eU versus K.

Units within the Longstaffe Bluff Formation (Table 1) are best distinguished by variation in mean K values, ranging from 2.3% and 2.4% for wacke, undivided psammite, and quartzitic (based on visual estimates of modal mineral compositions in the field) psammite, to 4.3% for semipelite units. Psammitic units with higher estimated biotite contents have higher K values (3.6%–3.7%) than other psammite units. Wacke units contain the highest mean eTh values (19.4 ppm) followed by the semipelitic units (16.1 ppm). Mean eTh values for the remaining psammite and quartzite units show a more limited range (13.7–14.6 ppm). Mean eU values show only a small increase from the biotite-poor units (3.5–3.6 ppm) to those units with higher estimated biotite contents and the wacke units (3.9–4.3 ppm).

The K and eTh concentrations for all measurements collected along the main transect through the central part of the Longstaffe Bluff Formation (A–D, Fig. 2) are shown in Figure 3. The separate field for the semipelite units based on their higher K values is clearly shown. The two psammitic units with higher biotite contents also plot separately, intermediate between undivided and quartzitic psammite, and the semipelite units. Variations in K values for the quartzite units and eTh values for the wacke units suggest two possible subfields for both. There appears to be a low-K quartzite and a low-eTh wacke, both of which plot in the same field as the undivided and quartzitic psammite units. Several high-eTh wacke units are

also evident in **Figure 3**. A number of measurements within undivided psammite overlap with biotitic psammite and semipelite. This overlap and the possible subfields for the quartzite and wacke units may reflect normal radioactive element variations for these units or errors associated with visual estimation of major mineral components. Some high-eTh psammite measurements overlap with the high-eTh wacke subfield, possibly reflecting increases in accessory minerals such as monazite, a common Th-bearing mineral. Excluding the wacke units, Figure 3 shows a generally positive correlation between increasing K values and increasing eTh values.

In **Table 2** and **Figure 4** results are presented from two traverses (E and F, **Fig. 2**) in the Flint Lake area. Measurements collected on muscovite schist, marble, and calc-silicate units are from the lower sequence of the Piling Group. All psammite measurements are from the Longstaffe Bluff Formation of the upper sequence. Quartzite and pelite-semipelite measurements from the lower and upper sequences were not plotted separately. An insufficient number of measurements were collected at these localities to determine if significant radioactive element variations exist between similar rock types in the lower and upper sequences of the Piling Group. Similar to results obtained along the main transect across the central part of the Longstaffe Bluff Formation (**Table 1**, Fig. 3), the radioactive element variations discriminate between psammitic and semipelitic units. The marble and muscovite schist units of the lower sequence of the Piling Group are also clearly discriminated; however, in this area, K (in particular), eU, and eTh concentrations vary considerably within the calc-silicate and quartzite units. Potassium values for four measurements from a 6–7 m thick calc-silicate unit range between 4.9% and 8.1%.

Values obtained for K, eU, and eTh concentrations in two Proterozoic (Corrigan et al., 2001) granite bodies south of Flint Lake are shown in **Figure 4** and summarized in **Table 2**. One is a large pegmatite intrusion (F, Fig. 2) and the other is a biotite syenogranite (E, Fig. 2). Values of eU and eTh for the biotite syenogranite average 11.6 ppm and 77.4 ppm, respectively, or about two times the Clark average for

uranium in a granite (Clark et al., 1966) and three times the Clark average for thorium. Mean eTh values for the pegmatite intrusion are strikingly different at only 5.5 ppm eTh or about one-quarter of the Clark value. These large differences in eTh values result in very different eU/eTh ratio values (**Fig. 4B**).

In **Table 3** and **Figure 5**, results for the five individual site locations (S1–S5, Fig. 2) are grouped separately by location to highlight regional differences between similar lithologies. Whereas additional measurements are required to more confidently define clear differences between the orthogneiss and various monzogranite and syenogranite bodies, Figures 5A and 5B do show variations in K, eU, and eTh concentrations that suggest mappable differences. The orthogneiss bodies have generally lower K and much lower eTh concentrations than most of the plutonic rocks. Values of eTh show the largest variations between plutonic rocks from different localities as well as between different lithologies at the same locality. Excluding the orthogneiss units and the high-K syenogranite at location S4, the large variation in eTh values and limited range in K values result in significant differences in the eTh/K ratio values. These variations can be used to identify and map lithological and elemental variations, sometimes cryptic, within and between composite intrusive suites.

DISCUSSION

While no airborne gamma-ray spectrometry data is yet available for the central Baffin Island region, some conclusions about potential utility of the technique for mapping and mineral exploration in this region can be made. A visual analysis of the reconnaissance, 5 km line-spaced, airborne gamma-ray spectrometry data from the southern Melville Peninsula with similar lithological units (Henderson, 1987) to those in central Baffin Island reveals a generally good correlation of the airborne data with various units of the Archean basement, despite the coarse line spacing. The airborne data clearly discriminates foliated, porphyritic to megacrystic granite from undifferentiated orthogneiss. The

occurrence of other anomalous radioactive element signatures in areas of undifferentiated orthogneiss might suggest the presence of additional, unmapped intrusive units. Variations between and within the different belts of Penrhyn Group supracrustal rocks are less obvious than those within the Archean basement units; however, some variations are evident where the different lithologies are sufficiently large to constitute a significant percentage of the spectrometer's field of view. Some of these differences are further enhanced by the distinct high eU, high eU/eTh, and low eTh signatures associated with aplitic to pegmatitic granitic rocks that intrude the Penrhyn Group. Uranium mineralization, first identified from the reconnaissance airborne gamma-ray spectrometry data, is associated with these pegmatitic plutons (Delpierre, 1982).

The results of this brief study have shown that increasing K concentrations are associated with increasing biotite contents in psammitic and semipelitic units of the Longstaffe Bluff Formation, that higher eTh concentrations are associated with some wacke units, and that discrimination between Archean orthogneiss and different Archean and Proterozoic intrusions is possible based on characteristic radioactive element signatures. The compositional differences within the supracrustal rocks of the Piling Group may be mappable using airborne gamma-ray spectrometry if the individual units are large enough or abundant enough to occupy a significant percentage of the airborne spectrometer's field of view. The radioactive element compositional differences reported here and generally larger dimensions for the various orthogneiss and intrusive units in the Archean basement north of the Piling Group suggest that these units can be delineated using airborne gamma-ray spectrometry. Provided these surveys are flown with sufficient flight-line density, the patterns would be expected to provide an important source of information in support of ongoing and future regional mapping and exploration activities in the central Baffin Island region. On the ground, the variations in K, eU, and eTh concentrations can be accurately and efficiently determined using a portable gamma-ray spectrometer, providing effective mapping and sampling guides at local, detailed scales.

Additional ground gamma-ray spectrometry studies are planned for the summer of 2001. The main focus of these studies will be the lower sequence of the Piling Group in and around Flint Lake and the Archean and Proterozoic intrusive rocks and Archean basement orthogneiss that occur north of the Piling Group.

ACKNOWLEDGMENTS

REFERENCES

Charbonneau, B.W., Holman, P.B., and Hetu, R.J.
1997: Airborne gamma spectrometer-magnetic-vlf survey of northeastern Alberta; *in* Exploring for Minerals in Alberta: Geological Survey of Canada-Alberta Agreement on Mineral Development (1992-1995); Geological Survey of Canada, Bulletin 500, p. 107–131.

Clark, S.P., Jr., Peterman, Z.E., and Heier, K.S.
1966: Abundance of uranium, thorium and potassium; *in* Handbook of Physical Constants, Geological Society of America, Memoir 97, p. 521–541.

Corrigan, D., Scott, D.J., and St-Onge, M.R.
2001: Geology of the northern margin of the Trans-Hudson Orogen (Foxe Fold Belt), central Baffin Island, Nunavut; Geological Survey of Canada, Current Research 2001-C23, 17 p.

Darnley, A.G. and Ford, K.L.
1989: Regional airborne gamma-ray surveys: A review; *in* Proceedings of Exploration '87, The Third Decennial International Conference on Geophysical and Geochemical Exploration For Minerals and Groundwater; (ed.) G.D. Garland, Toronto, Ontario; 27 September–1 October 1987, Ontario Geological Survey, Special Volume 3.

Delpierre, M.E.
1982: Anomaly '60': a uraniferous granitic pluton on Melville Peninsula, N.W.T.; *in* Uranium in Granites, (ed.) Y.T. Maurice; Geological Survey of Canada, Paper 81-23, p. 115–118.

Ford, K.L., Savard, M., Dessau, J.C., Pellerin, E., Charbonneau, B.W., and Shives, R.B.K.
in press: The role of gamma-ray spectrometry in radon risk evaluation: a case history from Oka, Quebec; GeoScience Canada.

Henderson, J.R.
1987: Geology, southeastern Melville Peninsula, District of Franklin, Northwest Territories; Geological Survey of Canada, Map 1655A, scale 1:100 000.

Holman, P.B., Carson, J.M., Ford, K.L., Grant, J.A., and Shives, R.B.K.
in press: Airborne gamma ray spectrometry compilation series – Quoich River, Nunavut; Geological Survey of Canada, Open File 4005.

Killeen, P.G.
1979: Gamma-ray spectrometric methods in uranium exploration - application and interpretation, p. 163–230; *in* Geophysics and Geochemistry in Search for Metallic Ores, (ed.) P.J. Hood; Geological Survey of Canada, Economic Geology Report 31, 811 p.

Mwenifumbo, C.J., Pflug, K.A., Elliot, B.E., Jefferson, C.W., Koch, R., Robbins, J., and Matthews, R.
2000: Multiparameter borehole geophysical logging at the Shea Creek and McArthur River projects: parameters for exploration, stratigraphy, and high-resolution seismic studies; *in* Summary of Investigations 2000, Volume 2; Saskatchewan Geological Survey, Saskatchewan Energy and Mines, Miscellaneous Report 2000-4.2.

Shives, R.B.K., Charbonneau, B.W., and Ford, K.L.
1997: The detection of potassic alteration by gamma-ray spectrometry – recognition of alteration related to mineralization; *in* Proceedings of Exploration 97: Fourth Decennial International Conference on Mineral Exploration, (ed.) A.G. Gubins; p. 741–752.

CURRENT RESEARCH
RECHERCHES EN COURS **2001**

Purchase Information

Information pour acheter

Titles Titres

Article

Article

Shives, R.B.K., Ford, K.L., and Charbonneau, B.W.
1995:   Applications of gamma-ray spectrometric/magnetic/VLF-EM surveys – Workshop Manual; Geological Survey of Canada, Open File 3061, 82 p.

**Wilford, J.R., Bierwirth, P.N., and Craig, M.A.**
1997:   Application of airborne gamma-ray spectrometry in soil/regolith mapping and applied geomorphology; *in* Australian Geological Survey Organisation Journal of Australian Geology & Geophysics, v. 17, no. 2, p. 201–216.

Geological Survey of Canada Project PS1006-KF

Figure 1. Ground gamma-ray spectrometry measurements on **A)** psammite of the Longstaffe Bluff Formation and **B)** marble of the Flint Lake Formation, lying between high-potassium calc-silicate unit (top) and muscovite schist (bottom). Both figures show the 2-pi geometry required for accurate gamma-ray spectrometry measurements.
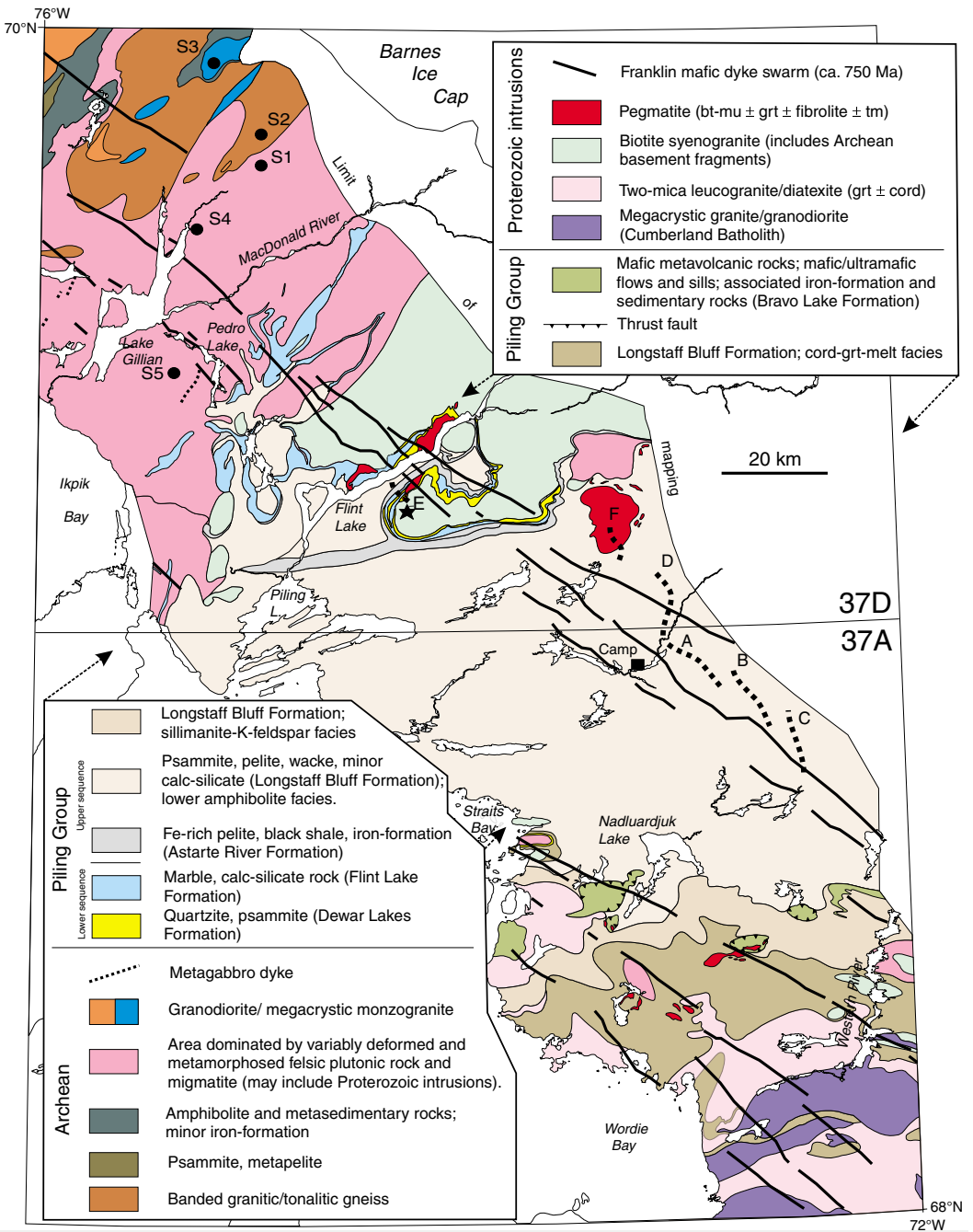
Figure 2. Simplified geological map of part of the Foxe Fold Belt, central Baffin Island from Corrigan et al. (2001) showing the location of gamma-ray spectrometry traverses (A–F) and sites (S1–S5); bt=biotite, mu=muscovite, grt=garnet, tm=tremolite, cord=cordierite.
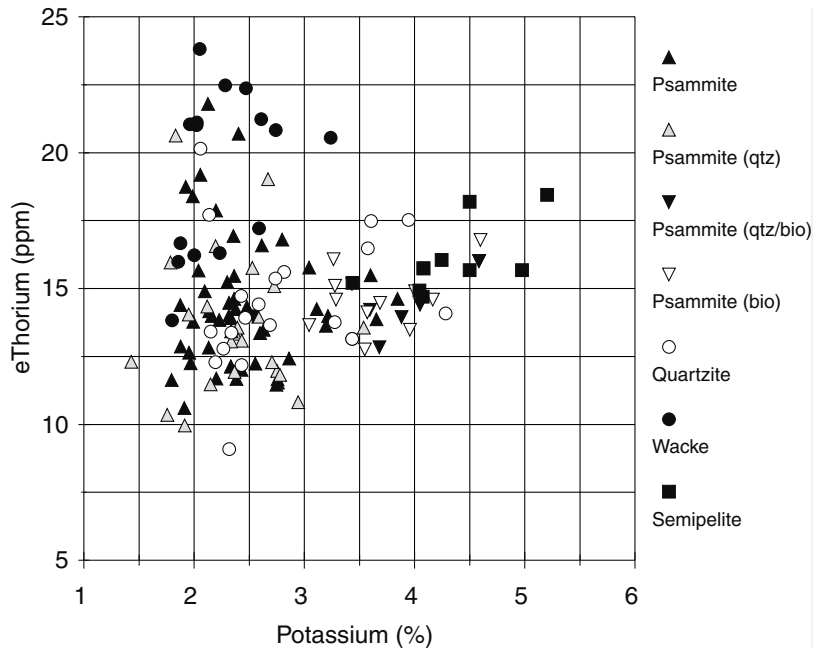
Figure 3. Radioactive element plot of eTh versus K for 134 ground gamma-ray spectrometry measurements across the central part of the Longstaffe Bluff Formation, Piling Group, central Baffin Island; qtz=quartz, bio=biotite.
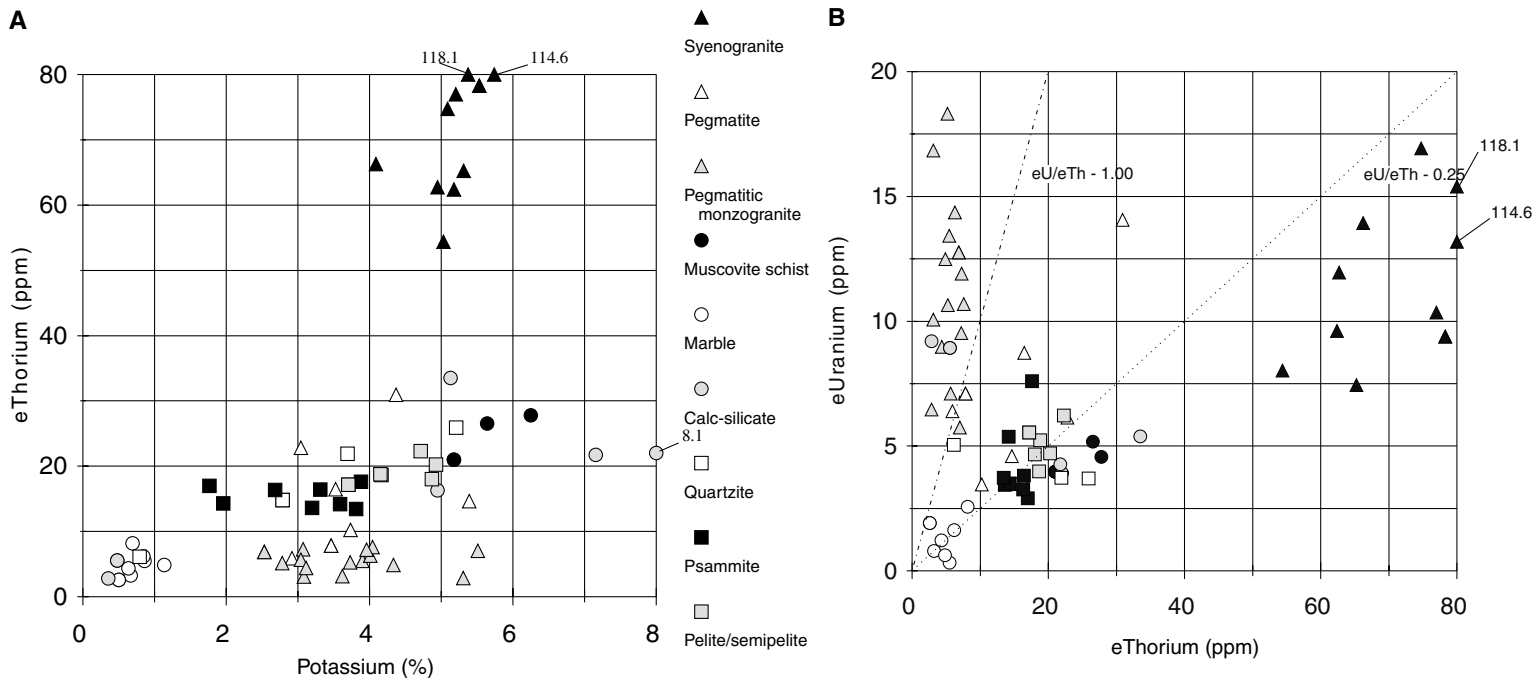
Figure 4. Radioactive element plots for 64 ground gamma-ray spectrometry measurements from the Flint Lake area, central Baffin Island.
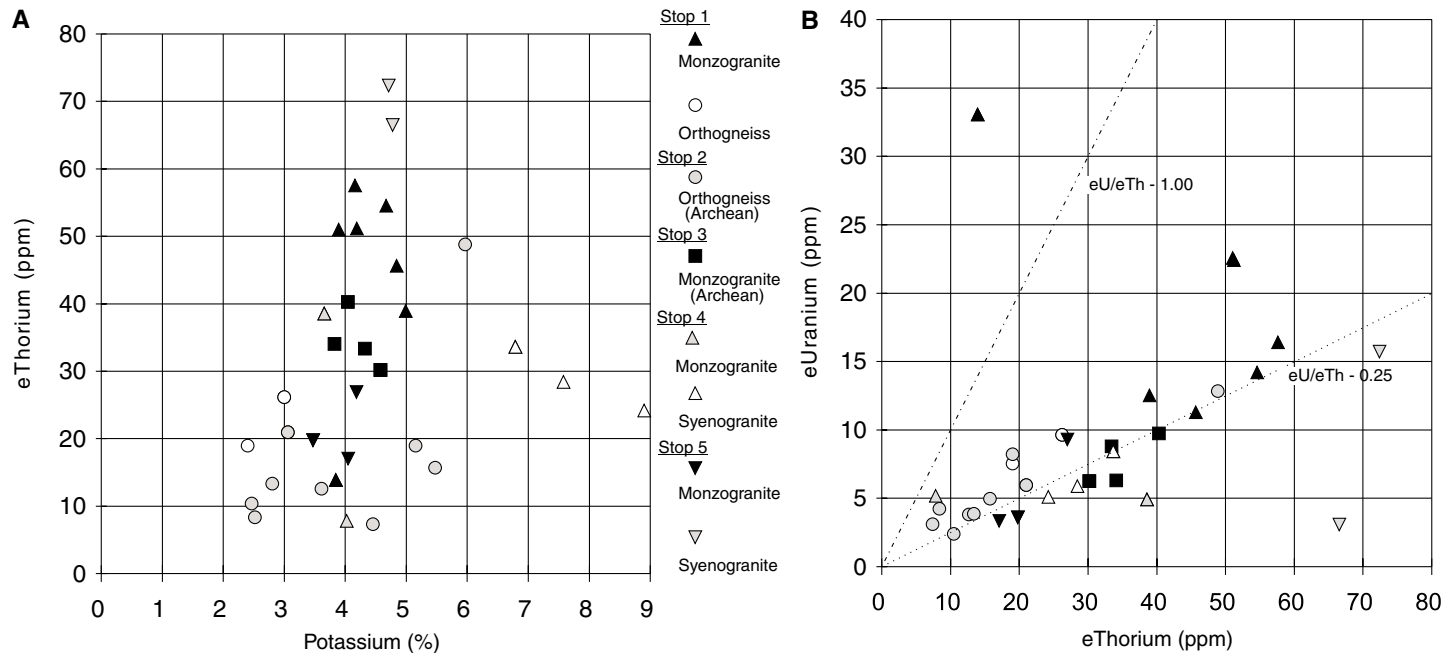
Figure 5. Radioactive element plots for 32 ground gamma-ray spectrometry measurements for granitic and gneissic lithologies from the MacDonald River and Drewry River areas, central Baffin Island.

Table 1. Radioactive element concentrations of the Longstaffe Bluff Formation, Piling Group, central Baffin Island as determined by in situ gamma-ray spectrometry.

Rock type	n	Potassium (%)			eUranium (ppm)			eThorium (ppm)		
		mean	SD	range	mean	SD	range	mean	SD	range
Psammite	48	2.4	0.5	1.8–3.8	3.5	0.8	1.4–6.3	14.4	2.4	10.6–21.8
Psammite (quartzitic)	24	2.4	0.4	1.4–3.5	3.5	0.9	2.1–6.5	13.7	2.5	10.0–20.6
Psammite (quartzitic/biotitic)	6	3.7	0.6	2.5–4.6	3.9	0.4	3.1–4.4	14.2	0.9	12.9–16.0
Psammite (biotitic)	12	3.6	0.4	3.0–4.6	4.0	0.7	2.6–5.0	14.6	1.0	12.8–16.8
Quartzite	20	2.8	0.6	2.1–4.3	3.6	0.8	2.1–4.9	14.6	2.4	9.1–20.2
Wacke	15	2.3	0.4	1.8–3.2	4.2	0.9	2.5–5.7	19.4	2.9	13.8–23.8
Semipelite	9	4.3	0.5	3.4–5.2	4.3	0.9	3.0–5.6	16.1	1.3	14.7–18.5

Table 2. Radioactive element concentrations of lithologies near Flint Lake, central Baffin Island as determined by in situ gamma-ray spectrometry.

Rock type	n	Potassium (%)			eUranium (ppm)			eThorium (ppm)		
		mean	SD	range	mean	SD	range	mean	SD	range
Syeno-granite	10	5.2	0.4	4.1–5.7	11.6	3.0	7.4–16.9	77.4	20.7	54.4–118.1
Pegmatite dykes	7	3.8	0.8	2.9–5.4	7.2	3.2	3.5–14.1	15.6	8.2	5.9–30.9
Pegmatitic monzogranite	15	3.7	0.8	2.5–5.5	11.3	3.5	5.8–18.3	5.5	1.5	2.9–7.6
Muscovite schist	3	5.7		5.2–6.2	4.6		4.0–5.2	25.1		21.0–27.8
Marble	7	0.8	0.2	0.5–1.1	1.3	0.7	0.3–2.6	5.0	1.7	2.6–8.2
Calc-silicate	4	6.3		4.9–8.0	4.2		3.4–5.4	23.4		16.4–33.6
Quartzite	4	3.1		0.8–5.2	4.0		3.5–5.1	17.2		6.14–25.9
Psammite	8	3.0	0.8	1.8–3.9	4.2	1.4	2.9–7.6	15.4	1.6	13.5–17.6
Pelite/semipelite	6	4.4	0.4	3.7–4.9	5.1	0.7	4.0–6.2	19.2	1.7	17.2–22.3

Table 3. Radioactive element concentrations of lithologies from the MacDonald River and Drewry River areas, central Baffin Island as determined by ground gamma-ray spectrometry.

		Potassium (%)			eUranium (ppm)			eThorium (ppm)		
Rock type	n	mean	SD	range	mean	SD	range	mean	SD	range
Monzogranite (stop 1)	7	4.4	0.4	3.8–5.0	18.9	7.1	11.3–33.1	44.7	13.8	13.9–57.6
Orthogneiss (stops 1 & 2)	11	3.7	1.2	2.4–6.0	6.1	3.0	2.4–12.9	18.4	11.1	7.4–48.9
Monzogranite (stop 3)	4	4.2		3.8–4.6	7.8		6.3–9.8	34.5		30.2–40.3
Monzogranite (stop 4)	2			3.7–4.0			4.9–5.2			7.8–38.6
Syenogranite (stop 4)	3	7.8		6.8–8.9	6.5		5.1–8.5	28.8		24.2–33.7
Monzogranite (stop 5)	3	3.9		3.5–4.2	5.4		3.4–9.3	21.3		17.1–27.0
Syenogranite (stop 5)	2			4.7–4.8			3.1–15.8			66.6–72.4